Research Article

Lixia Guo, Yanan Zhang, Ling Zhong*, Minghua Wang, and Xuanyi Zhu

Study on Macroscopic and Mesoscopic Mechanical Behavior of CSG based on Inversion of Mesoscopic Material Parameters

https://doi.org/10.1515/secm-2020-0007
Received Nov 04, 2019; accepted Feb 03, 2020

Abstract: Cement Sand and Gravel (CSG) is a low-cost, environment-friendly composite material mixed of unscreened aggregate, cement, fly ash and water, and its properties differ from ordinary concrete due to different aggregate characteristics. In order to investigate the effect of aggregate characteristics on the mechanical behavior of CSG, this paper used numerical simulation method to divide the CSG into aggregate unit, cement mortar unit and interface unit at the mesoscopic level and randomly generate aggregate, then used laboratory uniaxial compression test results to inverse the said mesoscopic component parameters, and finally verified the rationality of mesoscopic numerical simulation. Based on the inversed parameters, the numerical simulation test of different aggregate grading was carried out and analyzed. The results showed that: (1) From the perspective of macroscopic mechanical properties, as the sand ratio increased, the aggregate occupancy and the peak stress decreased; under the same aggregate occupancy (the same sand ratio), the stress peak became higher with the improvement of aggregate grading (aggregates of small particle size increased); (2) At the mesoscopic level, the crack of CSG usually appeared on the interface and around the aggregate; the smaller the sand ratio was, the higher the aggregate occupancy was, the more obvious the stress concentration was, and the earlier the cracking of the test piece was, but there were many aggregates, so the eventual failure time was delayed. These research results can provide theoretical basis for engineering design and construction.

Keywords: CSG, mesoscopic inverse analysis, mechanical behavior, cracking mechanism

***Corresponding Author: Ling Zhong:** North China University of Water Resources and Electric Power,Zhengzhou 450045, China; Academician workstation of water environment treatment and ecological restoration of Henan Province, Zhengzhou 450002; China; Key Laboratory of water environment simulation and treatment of Henan Province, Zhengzhou 450002, China; Email: 250514782@qq.com
Lixia Guo: North China University of Water Resources and Electric Power,Zhengzhou 450045, China; Academician workstation of water environment treatment and ecological restoration of Henan Province, Zhengzhou 450002; China; Key Laboratory of water environment simulation and treatment of Henan Province, Zhengzhou 450002, China
Yanan Zhang, Minghua Wang, Xuanyi Zhu: North China University of Water Resources and Electric Power,Zhengzhou 450045, China

1 Introduction

CSG is made of a few cementing materials (cement and fly ash) and a little water, mixed with the raw sand gravels in the natural river course. It features unscreened aggregates and less cementing materials (usually less than 100 kg/m^3) [1, 2], which makes it different from the conventional concrete. Therefore, it is necessary to make a study on the CSG characteristics, thus providing theoretical basis for engineering design.

Most previous researches used the experimental method, however, with the development of measurement technology and computer technology, the numerical simulation technology has been more used in the research of material characteristics.Wang Yongsheng [3] *et al.* conducted numerical simulation test research on indirect tensile strength of cement cold recycling mixtures by using particle flow code of two-dimension, Through laboratory test, inversion analysis reached the value of microscopic mechanical parameters, and verified the reliability of analysis simulation results. Li Chaohong *et al.* [4] made a mesoscopic numerical simulation of concrete damage and fracture process, and the compressive strength of the simulated cubic concrete was close to that measured in the test; Wang Jiang *et al.* [5] took into account the random distribution and shapes of aggregate, and concluded the damage distribution characteristics and macro stress-strain relationship of concrete under uniaxial tension through numerical analysis; Dang Nana *et al.* [6] used nonlinear finite element method to simulate the mesoscopic damage and fracture of the test piece, and obtained the macroscopic mechanical strength and failure process. It can be seen that the test process can be simulated through the numerical simulation, greatly saving project investment [7–10]. Many studies stay focused on the testing of CSG as a new material, while this paper investigates the effect of CSG aggregate on macroscopic and mesoscopic mechanical behavior of a dam toe by means of numerical simulation, based on the CSG's unscreened aggregate feature.

2 CSG characteristics

Because of the unscreened aggregate, the CSG is different from the conventional concrete. Figure 1 showed the grading and Fuller curves of 12 groups of sand gravels on the site of the CSG dam at Shoukoubao, Shanxi, from which, we could see that the grading of each group of sand gravels had a large deviation from the Fuller curve, indicating poor sand gravel grading at the project site. Calculated based on the grading of the said 12 groups of CSG, the average sand ratio was 41.8%.

During the mix design of CSG, a sand ratio selection test is generally adopted to obtain a proper range of sand ratios, then a test on whether the consumption and strength of cementing materials meet the design requirements is carried out, and finally an appropriate mix proportion of cementing material consumption and sand ratio is proposed. It can be seen that the mix design of CSG requires a large number of tests, and the tests consume a lot of manpower and material resources. however, if the numerical simulation method is used, the number of tests can be greatly reduced, thereby saving engineering investment.

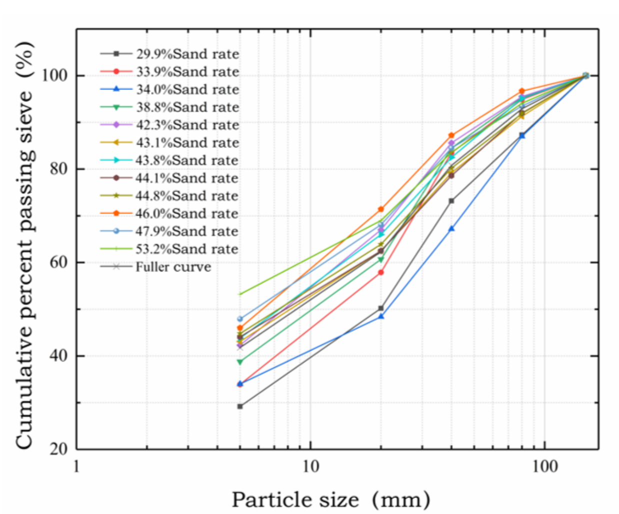

Figure 1: 12 Gravel Gradation and Fuller Curve

3 Random aggregate model

CSG is composed of unscreened aggregate, cementing material and water. From a mesoscopic perspective, CSG can be regarded as a three-phase composite material consisting of natural sand gravel aggregate, mortar matrix, and interface between the mortar matrix and the aggregate. When a random aggregate model is used for finite element numerical analysis, the finite element model is divided into aggregate unit, cement mortar unit and interface unit at a mesoscopic level.

3.1 Random aggregate generation

The aggregate particles are randomly distributed on the cross section of the test piece with the help of the pseudo random numbers generated by the Monte Carlo method [11–14]. In computer simulation, the fundamental random variables were those uniformly distributed within the interval [0,1]. The probability density function with **X** was:

$$f(x) = \begin{cases} 1 & x \in [0, 1] \\ 0 & x \notin [0, 1] \end{cases} \quad (1)$$

A sampling sequence $[x_1, \ldots, x_n]$ of the random variable **X** can be generated in the computer. The random variables uniformly distributed within the interval [0,1] were the fundamental random variables, and based on them, the random variables in other distribution forms can also be obtained. For example, a random variable x' uniformly distributed within the interval [a,b] can be obtained by transforming $x' = a + (b - a)x$. Similarly, the random numbers of random variables in other distribution forms can also be obtained by transformation of random numbers of random variables uniformly distributed in the interval [0,1].

Monte Carlo method was used to randomly determine the location of aggregates of various particle sizes in the test piece. As to the number of aggregate particles, the method of Walraven *et al.* [15] was used to convert the three-dimensional aggregate grading curve into the probability of occurrence of aggregates of any diameter in a two-dimensional plane. The probability $P_c(D < D_0)$ of aggregates with diameter $D < D_0$ at any point in the two-dimensional plane was

$$P_c(D < D_0) = P_k\left[1.065\left(\frac{D_0}{D_{\max}}\right)^{0.5} - 0.053\left(\frac{D_0}{D_{\max}}\right)^{4} - 0.012\left(\frac{D_0}{D_{\max}}\right)^{6} - 0.0045\left(\frac{D_0}{D_{\max}}\right)^{8} - 0.0025\left(\frac{D_0}{D_{\max}}\right)^{10}\right] \quad (2)$$

In formula (2), D_0 was the mesh diameter; D_m was the maximum aggregate particle size; P_k was the percentage of the aggregate volume to the total volume of the test piece, generally 75%.

The probability distribution curve was obtained according to the formula (1), based on which, the number of aggregates of different particle size on the cross section of the test piece was obtained. The aggregates were substantially convex and can be simplified into irregular polygons. The specific steps were as follows: 1. Determine the required number of aggregates of different particle size according to the aggregate grading curve; 2. Generate random circles of the aggregates and random circles of the cementing belt boundaries; 3. Divide quadrants in the circles inside and outside, determine the number of corner points in each quadrant and generate the coordinates of the corner points; 4. Connect the corner points to generate a polygon.

3.2 Constitutive model

From a mesoscopic perspective, CSG consists of two materials and one interface namely aggregate, cement mortar of different sand ratios and interface between the aggregate and the cement mortar. Therefore, the random polygon aggregate model included three units: sand gravel aggregate unit, mortar unit, and interface unit. To simplify the calculation, the constitutive relation and failure criterion of the mesoscopic components generally selected a simple form: the constitutive model adopted the linear elastic model [16–25], the constitutive equation is

$$\sigma = E\varepsilon \quad (3)$$

Where E the modulus of elasticity.

And the failure criterion adopted the theory of maximum tensile stress, that is, when the maximum tensile stress exceeds the tensile strength, the material cracks [26, 27].

3.3 Mesoscopic material parameters and their inverse analysis

3.3.1 Mesoscopic material parameters

Since the constitutive model of each constituent material used linear elastic model, the material parameters included tensile strength, elastic modulus and Poisson's ratio. The aggregate of CSG is mostly pebbles or gravels with the particle size of less than 150 mm. As to the mesoscopic parameters of the aggregates [28–30], the existing reports mostly took macroscopic values, and it was reported [31] that: the rock parameters were affected by the size, the elastic modulus decreased with the increase in size, the strength increased with the increase in size, and the Poisson's ratio remained essentially unchanged. The CSG aggregate was small in particle size and diverse in shape. Due to the limitation of testing methods, it was hard to obtain the actual parameters of the aggregate particles. This paper used inverse analysis to obtain the actual parameters of aggregate particles and the elastic modulus of interface materials and mortar matrix.

The failure criterion of mesoscopic components adopted the maximum tensile stress criterion, with reference to the pertinent literature [32–35], and the values were shown in Table 1.

Table 1: Tensile strength and Poisson's ratio of meso-components

Meso component	tensile strength/MPa	Poisson's ratio
Cement mortar	2.8	0.25
Interface	1.5	0.3
aggregate	4.8	0.15

3.3.2 Inverse analysis

Contrary to the normal analysis, the inverse analysis is to deduce the mesoscopic parameters by inversion based on the laboratory macroscopic test results. The parametric inversion optimization used genetic algorithm and was realized through the data transmission between MATLAB and finite element software. The realization process was as follows: (1) Generate the initial parameter population through MATLAB, namely the parameters required for mesoscopic numerical simulation; (2) Read the generated data file into the finite element software for uniaxial compression test and simulation analysis, and output the numerical simulation result; (3) MATLAB read the numerical simulation results file, and compared it with the laboratory uniaxial compression test result to judge whether the iteration was stopped. If the accuracy met requirements, the algorithm ended. If failed, a new population was re-selected and cross-generated. Repeat (2)-(3) until an optimal solution was obtained.

Figure 4 showed a photo of a damaged cubic CSG after laboratory uniaxial compression. The size was 100mm*100mm*100mm, and the aggregate was of standard second grade, as shown in Table 2. "*d*" expressed the particle size and "*w*" the particle composition.

Table 2: Particle size distribution after aggregate screening

d/mm	w/%	d/mm	w/%
>35~40	6.1	>10~20	27.27
>20~35	57.58	>5~10	9.1

The mix proportion of the CSG was shown in Table 4.

The laboratory uniaxial compression test used a universal testing machine and a displacement control method. The displacement was controlled with different load steps, which corresponded to different stresses, and thus a stress-strain curve was obtained according to the laboratory measurements. In the numerical simulation analysis, a screened second-grade wet aggregate was adopted, with the boundary conditions of full constraints at the bottom and no constraints at the top, which were detailed in the lower right corner of Figure 2; when the genetic algorithm was used for the inverse analysis, the crossover probability was taken as 70%, and the mutation probability 10%. The objective function was:

$$\min J = \sum_{k=1}^{N} \left[\sigma^{j}{}_{k} - \sigma_k^m\right]^2 \tag{4}$$

Where: σ_k^j was the calculated value of the stress corresponding to the k-th load step, σ_k^m was the experimental value of the stress corresponding to the k-th load step, and N was the total number of load steps, controlled by the total displacement.

After 16 iterative solutions, the elastic modulus of the aggregate in identified CSG by inversion was finalized as E_G = 500Mpa, the elastic modulus of the mortar matrix E_m = 30Mpa, and the elastic modulus of the interface E_i = 20Mpa. The numerical simulation results and test results were shown in Figure 2.

Through the analysis of parametric inversion results, the stress peak in the laboratory test was slightly lower than that in the numerical simulation due to the test conditions, aggregate characteristics, mixing process and other factors, while the strain values were basically the same; thus, their correlation coefficient was very high.

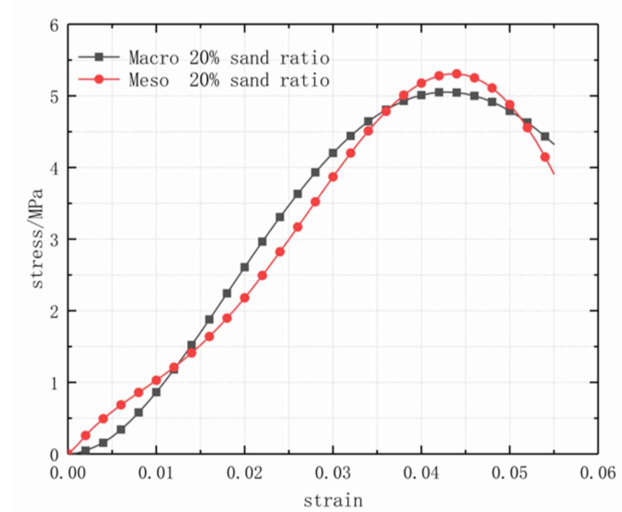

Figure 2: Analysis of parameters inversion results

4 Analysis on macroscopic and mesoscopic mechanical behavior of CSG

4.1 Compression test simulation

We carried out a numerical simulation test on 100*100*100 CSG of different aggregate grades to investigate the effect of grading. In the calculation, the mesoscopic material parameters were assumed unchanged, see Section 2.3, and the aggregates of 30 mm or more were removed in order to compare with the laboratory test results of the screened wet test block. The sand ratios selected were 18.5% (Fuller standard), 34.0%, 43.1% and 46.0% respectively. According to the random aggregate generated and its interface in 2.1 , the material numbers of aggregate, interface and mortar are determined based on the surface number, the corresponding material numbers are assigned to the corresponding material parameters in ANSYS, after grid division, and the established random aggregate models were shown in Figure 3 (a, b, c and d). If the grading of aggregates on the site was poor, the large aggregates could be crushed to improve the grading; therefore, 34.0% and 43.1% were added in the simulation test as control groups. In the control groups, the number of aggregates of small particle size was increased and the number of aggregates

Table 3: Some project mix proportion

Cement (kg/m^3)	Flyash (kg/m^3)	Sand (kg/m^3)	Water (kg/m^3)	aggregate (kg/m^3)	Sand rate
70	20	434	90	1736	0.2

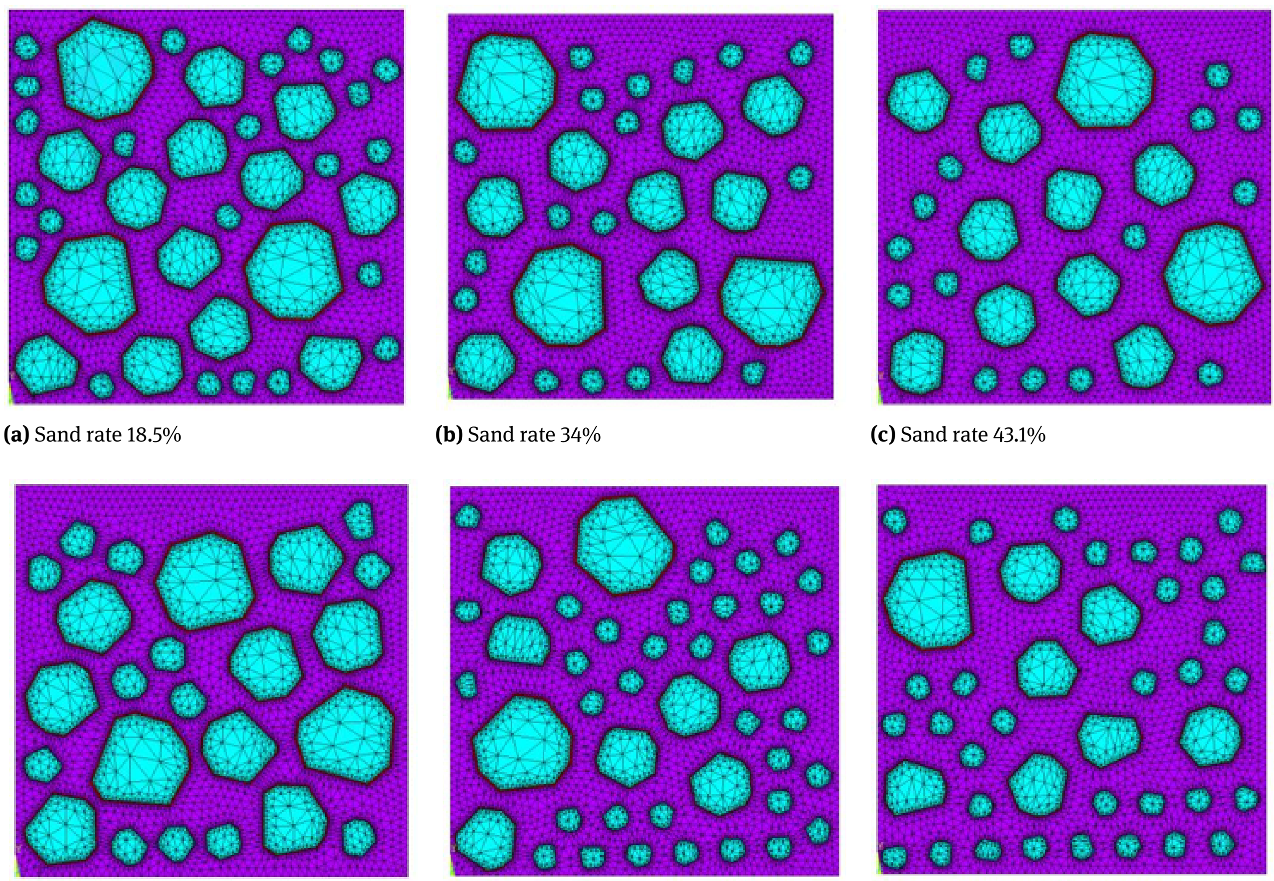

(a) Sand rate 18.5% **(b)** Sand rate 34% **(c)** Sand rate 43.1%

(d) Sand rate 46% **(e)** Sand rate 34% control group **(f)** Sand rate 43.1% control group

Figure 3: Random aggregate model

of large particle size was reduced under the condition that the total number of aggregates kept unchanged. The models were shown in Figure 3 (e, f).

4.2 Results analysis

4.2.1 Analysis of macroscopic mechanical behavior

The uniaxial compression simulation test used displacement loading to obtain a stress-strain curve. Figure 4(a) showed the stress-strain curves at different sand ratios; Figure 4(b) showed the stress-strain curves at different grades with the same sand ratio.

In Figure 4(a), with the increase of the sand ratio, the aggregate occupancy and the peak stress decreased, indicating an inverse relation between the sand ratio and the peak stress, which was consistent with the conclusion in the literature [36]; as the sand ratio increased, the slope of tangent of the stress-strain curve decreased, that was, the elastic modulus became smaller. It was because that with the increase of sand ratio, the aggregate occupancy decreased, and the mechanical properties of the CSG were affected more by the mortar matrix and less by the aggregate; thus the strength and the elastic modulus were both reduced.

In Figure 4(b), under the same aggregate occupancy (the same sand ratio), as the aggregate grading was improved (the aggregates of small particle size increased),

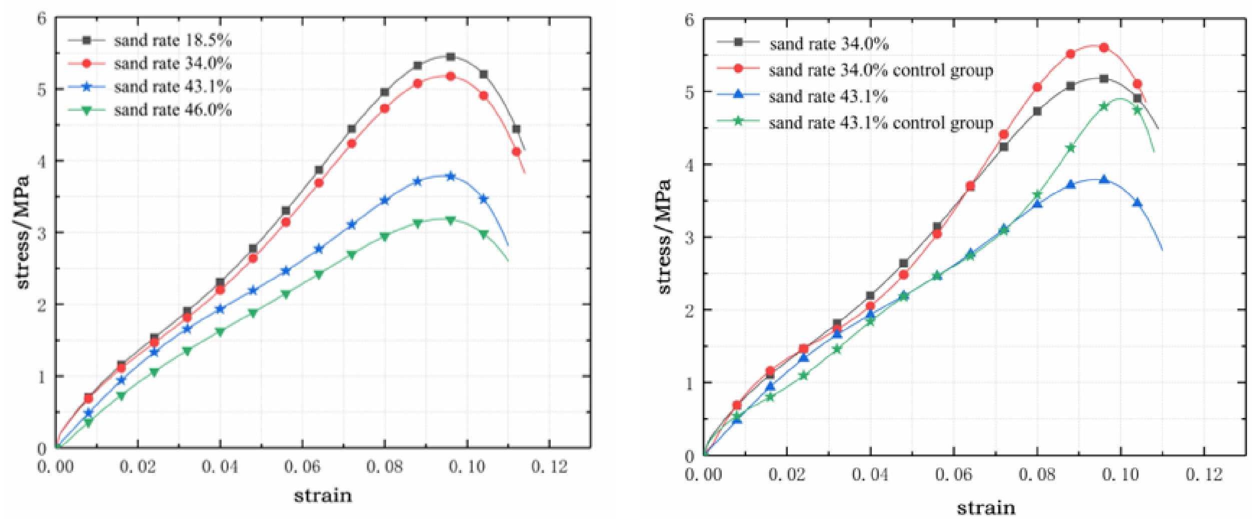

(a) Stress-strain curves at different sand rates

(b) Different aggregate size at the same sand rate

Figure 4: Simulated stress-strain curve of uniaxial compression

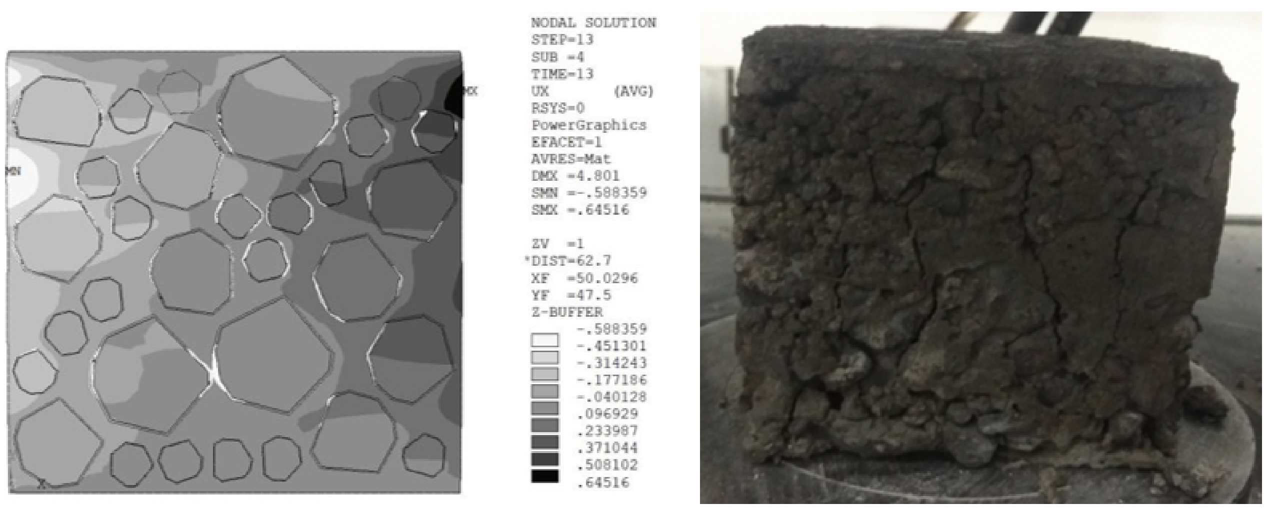

(a) Meso-damage

(b) Macro-destruction

Figure 5: Macro-meso damage contrast chart

the stress peak became higher, and vice versa. It was because that the elastic modulus of the aggregate and the cement mortar was different, leading to inconsistent deformation, and if the grading was worse, the stress concentration was more obvious, resulting in lower strength of CSG overall. This result can provide guidance for the on-site construction.

4.2.2 Analysis of macroscopic and mesoscopic damage mechanism

Figure 5 showed the damaged test blocks of 20% sand ratio and standard second grade in the numerical simulation and the laboratory test.

Through comparison between Figure 5(a) and (b), the white part in (a) was the crack after damaged, mostly located in the transition zone between the mortar matrix and the aggregate and a few in the mortar matrix and around the aggregate, which was consistent with (b) in terms of the cracking site and the cracking rule. It was because that the aggregate and the mortar matrix were different in characteristics, resulting in inconsistent deformation (see (a), the displacement was uneven along the aggregate distribution), the stress was concentrated near the aggregate, and the strength at the interface of transition zone between the mortar matrix and the aggregate was the lowest due to the micro-cracks; therefore, the micro-cracks were easier to appear on the transition zone [37], and as the load increased, the energy would release from the weakest point and then extend to the mortar matrix, and the crack bypassed the aggregate to expand along the interface.

After the test block was loaded, the elasticity deformed first, and with the pressure increase, some of the mesoscopic components began to rupture. Table 4 showed the initial failure load step and the eventual failure load step at different sand ratios.

Table 4: Analysis of failure of specimens

Model type	Start the failure load step (step)	Complete Failure Load Step (step)
Model a	8	15
Model b	9	15
Model c	10	13
Model d	10	13
Sand rate 20%	8	15

It could be seen from Table 4 that: under the same mix proportion, the smaller the sand ratio of the CSG was, the higher the aggregate occupancy was, causing more obvious stress concentration. The low strength of the mortar matrix resulted in earlier cracking of the test piece; the high strength of the aggregate led to strong bearing capacity of the test piece and later eventual failure. On the contrary, the higher the sand ratio was, the lower the aggregate occupancy was, resulting in later cracking and earlier eventual failure.

5 Conclusion

By analyzing the aggregate characteristics of CSG, establishing two-dimensional random polygon aggregate models and calling of MATLAB and calculation software, this paper realized the inverse analysis of the mesoscopic component parameters, and the results were consistent with the test results. According to the typical characteristics of aggregates on the project site, this paper analyzed the effects of aggregate grading on the macroscopic and mesoscopic properties of CSG through mesoscopic numerical simulation, and came to the following conclusions:

1. With the increase of the sand ratio, the aggregate occupancy and the peak stress decreased, indicating an inverse relation between the sand ratio and the peak stress; as the sand ratio increased, the slope of tangent of the stress-strain curve decreased, that was, the elastic modulus became smaller. Under the same aggregate occupancy (the same sand ratio), as the aggregate grading was improved (the aggregates of small particle size increased), the stress peak became higher, and vice versa. This result can provide guidance for the on-site construction.
2. The cracks of CSG mostly appeared at the transition zone between the aggregate and the mortar matrix and around the aggregate. The smaller the sand ratio was, the higher the aggregate occupancy was, the more obvious the stress concentration was, and the earlier the cracking of the test piece was, but there were many aggregates, so the eventual failure time was delayed; the higher the sand ratio was, the lower the aggregate occupancy was, resulting in later cracking and earlier eventual failure.

References

[1] Jia JS, Ma FL, Li XY. Study on material characteristics of cement-sand-gravel dam and engineering application. J Hydraul Eng. 2006;37(5):578–82.
[2] Feng W, Jia JS, Ma FL. Study on durability of dam materials and new-type protective materials for cemented sand and gravel dam. J Hydraul Eng. 2013;44(4):500–4.
[3] Wang YS, Liu YJ. Simulation of indirect tensile strength of cold recycled cement mixture by two-dimensional particle flow software. JCCS. 2019;47(11):1611–20.
[4] Li CH, Wang HL, Xu GX. Three dimensional mesoscopic numerical simulation of concrete damage and fracture. J Cent South Univ. 2011;42(02):463–9.
[5] Wang J, Xu B, Chen HB. Numerical simulation of multi-scale homogenization of concrete tensile properties. CHIN J APPL MECH. 2019;36(03):538–46.
[6] Dang NN, Peng YY, Zhou HP, Cheng J. Micro damage analysis method of recycled concrete based on random aggregate model. Guti Lixue Xuebao. 2013;33 S1:58–62.
[7] Multi-scale computational models for the simulation of concrete materials and structures. In: Cusatis G, Rezakhani R, Alnaggar M. Proceedings of EURO-C 2014 Conference. London, UK:Taylor & Francis Group; 2014:23-38.
[8] Sun B, Li Z. Multi-scale modeling and trans-level simulation from material meso-damage to structural failure of reinforced concrete frame structures under seismic loading. J COMPUT SCI-NETH. 2016;12:38–50.

[9] Tian HW, Zhou Z, Lu JP, Peng Z. Micro Numerical Simulation of axial compression performance of fiber reinforced resin composite confined ultra-high performance concrete. J COMPOS MATER [Internet]. 2019 Aug [cited 2020 Feb 18]; 001:[about 2 p.]. Available from: https://doi.org/https://doi.org/10.13801/j.cnki.fhclxb
[10] Song LZ, Shen T. Meso numerical simulation of failure characteristics of foam concrete under uniaxial compression. B CHIN CERAM SOC. 2019;38(06):1823–31.
[11] Bai W, Peng G. ANSYS implementation of Monte Carlo method to generate random aggregate model of concrete. Shihezi Daxue Xuebao Ziran Kexue Ban. 2007;(04):504–7.
[12] Xu ZJ. Monte Carlo method. 1st ed. Shanghai Science and Technology Press; 1985.
[13] Rong MD, Guo ZY, Wu XQ. ANSYS implementation of two-dimensional and three-dimensional random aggregate model generated by Monte Carlo method. Construction Machinery Technology & Management. 2017;30(11):71–3.
[14] Li ZW. Monte Carlo simulation of related random variables. Stat Decis. 2007;(05):9–10.
[15] Schlangen E, VanMier GM. Simple lattice model for numerical simulation of fracture of concrete materials and structures. Mater Struct. 1992;25(9):534–42.
[16] Baznt ZP, Ožbolt J; BAŽANT Z P. OZBOLT J. Nonlocal microplane model for fracture, damage, and size effect in structures. J Eng Mech. 1990;116(11):2485–505.
[17] Zhu WC, Teng JG, Tang CA. Numerical simulation of strength envelope and fracture patterns of concrete under biaxial loadin. MAG CONCRETE RES. 2002;54(6):395–409.
[18] Zhu WC, Tang CA, Wang SY. Numerical study on the influence of meso-mechanical properties on macroscopic fracture of concrete. Struct Eng Mech. 2005;19(5):519–33.
[19] Tang CA, Zhang YB, Liang ZZ, Xu T, Tham LG, Lindqvist PA, *et al.* Fracture spacing in layered materials and pattern transition from parallel to polygonal fractures. Phys Rev E Stat Nonlin Soft Matter Phys. 2006 May;73(5 Pt 2):056120.
[20] Xu Q, Zhou XS, Cheng ZC. Random aggregate model and micromechanics analysis of concrete based on ANSYS. Engineering Journal of Wuhan University. 2019;52(12):1035-1040+1047.
[21] Li D, Jin L, Du XL, Liu JB, Zhang S, Yu WX. Theoretical prediction model of macro mechanical properties of concrete considering the influence of micro components. ENG PLAST APPL. 2019;36(05):67–75.
[22] Du XL, Jin L. Application of micro analysis method in the study of physical / mechanical properties of concrete. J Hydraul Eng. 2016;47(03):355–71.
[23] Correlation analysis of concrete microstructure and mechanical characteristics based on random aggregate model[dissertation]. Heibei: Hebei University of engineering;2019.
[24] Study on meso mechanical model of concrete based on random aggregate [dissertation]. Wuhan: Wuhan University of science and technology;2019.
[25] Li J, Yang WZ. Study on elastoplastic random damage constitutive relation of concrete. KSCE J Civ Eng. 2009;42(02):31–8.
[26] Yu XZ, Ju X. strength and failure of concrete. J Hydraul Eng. 1983;(02):22–36.
[27] Comi C, Perego U. Fracture energy based bi-dissipative damage model for concrete. Int J Solids Struct. 2001;38(36):6427–554.
[28] Wang LS, Sun DS, Zheng XH, Zhao WH, Li AW, Li Q. Experimental study on size effect of uniaxial compressive strength of three typical rocks. J Geom. 2017;23(02):327–32.
[29] Jin L, Li XR, Du XL, Fan LL. Size effect of GFRP on axial compressive strength of concrete cylinder: a meso analysis. J Hydraul Eng. 2019;50(04):409–19.
[30] Li D, Jin L, Du XL, Liu JB. Theoretical prediction method of concrete mechanical properties considering the effect of material hierarchical size effect. J Hydraul Eng. 2018;49(04):464–73.
[31] Tang DM, Yang SC. Study on size effect of rock uniaxial compressive strength. Sichuan Water Power. 2011;30(S1):119-122+126+156.
[32] Xiao JZ. Experimental study on stress-strain curve of recycled concrete under uniaxial compression. J TONGI UNIV :ENG SCI ED. 2007;(11):1445–9.
[33] Peng YJ, Wang YH. Numerical analysis of concrete fracture process and failure mechanism based on meso level. China Safety Science Journal. 2006;(08):110–4.
[34] Shang XL, Yang JW, Li JS. Fractal characteristics of micro fracture cracks of recycled concrete based on CT image. J Compos Mater. 2019;•••:1–11.
[35] Jin L, Hao HM, Zhang RB, Du XL. Meso numerical analysis of high temperature dynamic splitting behavior of concrete. ENG PLAST APPL; 2019. pp. 1–13.
[36] Research and engineering application of material characteristics of cemented sand gravel dam[dissertation]. Beijing:China Academy of water resources and hydropower; 2013.
[37] Xiao JZ, Li WG, Liu Q. Meso numerical simulation of uniaxial compression performance of recycled concrete model. J TONGI UNIV :ENG SCI ED. 2011;39(06):791–7.